

## GREEN SYNTHESIS OF SILVER NANOPARTICLES USING FRUIT EXTRACT OF *MALUS DOMESTICA* AND STUDY OF ITS ANTIMICROBIAL ACTIVITY

K. ROY<sup>a, b \*</sup>, C. K. SARKAR<sup>b</sup>, C. K. GHOSH<sup>a</sup>

<sup>a</sup>*School of Materials Science and Nanotechnology, Jadavpur University, Kolkata-700032, India*

<sup>b</sup>*Department of Electronics and Telecommunication Engineering, Jadavpur University, Kolkata-700032, India*

The green synthesis route, in comparison to the conventional chemical and physical procedures, is an easy and eco-friendly alternative to synthesize metallic nanoparticles. Here, we report a cost-effective, clean and fast bio-process to synthesize Ag nanoparticles after reduction of Ag<sup>+</sup> using apple (*Malus domestica*) fruit extract. The formation of silver nanoparticles was first examined by UV-Vis spectroscopy. Different phases and morphology of Ag nanoparticles were analyzed by X-ray diffraction and transmission electron microscopy respectively. Fourier transform infrared spectroscopy was used to identify the biomolecules responsible for reduction and stabilization of Ag nanoparticles. Antimicrobial property of our synthesized Ag nanoparticles was tested against three common bacteria- *Staphylococcus aureus*, *Klebsiella pneumoniae* and *Escherichia coli* and two fungi- *Aspergillus niger* and *Aspergillus wentii* by conventional disc diffusion procedure. The inhibition zone, formed on the discs in presence of silver nanoparticles, proved effective antimicrobial property of these nanoparticles against the tested bacterial and fungal strains.

(Received July 15, 2014; Accepted September 17, 2014)

**Keywords:** Silver nanoparticles, apple (*Malus domestica*) fruit extract, UV-Vis Spectroscopy, XRD, TEM, antimicrobial activity

### 1. Introduction

Over the past few decades, research on nanomaterials has received considerable attention in the field of catalysis, water treatment, biotechnology, biosensor etc. due to their versatile physicochemical properties (1, 2). It has been well established that the properties of the nanomaterials are determined by their size, shape, composition and crystallinity (3). Among different nanomaterials developed so far, nanomaterials of novel metals have established their potentiality in many fields due to their various unique properties like high electrical conductivity, chemical stability, anti-microbial activity etc (4). In this context, particularly Ag nanoparticles are well known for potential applications in the field of medicine technology including drug delivery, antibacterial activity etc. Research activity that has already been carried out on Ag nanoparticles reveals that they possess high antibacterial activity against Gram-negative as well as Gram-positive bacteria and antiviral activity against HIV-1 virus, respiratory syncytial virus, hepatitis B virus etc (5). Over the years, several routes such as conventional chemical reduction (6), electrochemical methods (7), photocatalytic reactions (8), laser ablation (9), micro-wave assisted methods (10) and most recently biological green routes (11, 12) have been developed as an initial step of research to synthesis Ag nanoparticles in a wide range of particle size. Among them, green route offers several advantages over the existing physical and chemical methods as it is simple, clean and eco-friendly. Use of marine algae (13,14), fungi (15-17) and bacteria (18-20) for synthesis of Ag nanoparticle is quite common but the use of extracts (21-23) of different parts of

---

\*Corresponding author: lordkaushikroy@gmail.com

plants cuts down the level of cost of the synthesis and doesn't involve any special isolation or complicated strain culture as well.

After detail review of current literature on biosynthesis of nanoparticles using green chemistry, it may be concluded that the leaf extracts of various plants are frequently used for synthesis of Ag nanoparticles (24-27) due to the presence of reducing agents within their leaves. But use of the fruit extract may also be a novel alternative for this purpose and was adopted by a few researchers in recent past including us (28-30). For example, Roy et al. synthesized silver nanoparticles from silver salt using fruit extract of grapes (*Vitis vinifera*) (28). Jain et al. showed that the fruit extract of Papaya (*Carica papaya*) can also be used to prepare silver nanoparticles from silver nitrate solution (29). Issac et al. reported the synthesis of gold and silver nanoparticles from chloroauric acid and silver nitrate respectively using the fruit extract of *Averrhoa bilimbi* (30).

In this paper, we have reported for the first time, the synthesis of Ag nanoparticles by reducing silver ions in the presence of fruit extract of apple (*Malus domestica*). Later, the antibacterial activity of silver nanoparticles has been carried out against one gram positive bacteria - *Staphylococcus aureus*, two gram negative bacteria - *Klebsiella pneumoniae* and *Escherichia coli* and two fungi - *Aspergillus niger* and *Aspergillus wentii*.

## 2. Experimental Details

### 2.1. Materials

To prepare the fruit extract of apple (Figure 1), fresh apples were collected from local market. Pure silver nitrate ( $\text{AgNO}_3$ ) used in this work was purchased from Merck India Ltd. The cultures of bacteria strains - *Staphylococcus aureus*, *Klebsiella pneumoniae* and *Escherichia coli* and fungal strains- *Aspergillus niger* and *Aspergillus wentii* were purchased from National Chemical Laboratory, Pune, India. Nutrient agar and potato dextrose agar used for antimicrobial study were purchased from Himedia, India.



Fig. 1. Fresh apple (*Malus domestica*)

### 2.2. Methods

#### 2.2.1. Synthesis of silver nanoparticles

For the preparation of apple fruit extract, a fresh and clean apple (weight around 50g) was cut into small pieces and crushed inside a grinder. Then it was centrifuged at 3,000 rpm for 10 minutes and filtered to obtain the pure and liquid fruit extract of apple. 20 mM stock solution of silver nitrate was prepared by dissolving 0.34g  $\text{AgNO}_3$  in 100 ml deionized water. To reduce silver ions, 10 ml of fruit extract was added drop wise to the above mentioned solution of silver nitrate so that the resulting mixture became half-diluted (resulting concentration 10 mM). In order to examine the effect of  $\text{AgNO}_3$  concentration upon the rate of Ag nanoparticles formation, we have carried out the same experiment using three different concentrations 3, 5, and 15 mM. To separate

the nanoparticles from the mixture, solution was centrifuged again at 20,000 rpm for 60 minutes. The soup was decanted and the supernatant precipitate was re-dispersed in 15 ml deionized water. After washing the residue several times using DI water, it was again centrifuged at 20,000 rpm for 30 minutes to remove the biomass completely. The precipitate, formed at the bottom of centrifugation tube, was collected carefully and dried in high vacuum to obtain dry powder that was used for further characterizations.

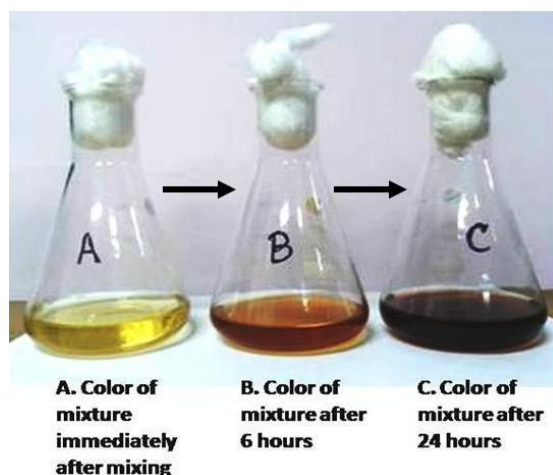


Fig. 2. Color change indicates formation of silver nanoparticles

### 2.2.2. Characterization of Ag-nanoparticles

Optical investigation was performed by UV-Vis spectroscopy using Perkin Elmer spectrophotometer in the wavelength range between 300 and 700 nm. Vacuum dried precipitate was investigated by x-ray diffractometer (XRD, Rigaku, Ultima – III, Japan) to confirm the proper phase of the precipitate. The x-ray diffractometer having an operating voltage 40 kV with Bragg-Brentano geometry and Cu  $K_{\alpha}$  radiation ( $\lambda = 0.154$  nm) as a source of radiation was used for measurement. Transmission electron microscope (JEOL-2010, USA, 200kV) was used to investigate microstructure of the synthesized nanoparticles. To prepare the sample for this analysis, the dry powder was suspended in deionized water maintaining a standard concentration 50 $\mu$ g/ml. Then a drop of this suspension was placed on the carbon-coated copper grid and the grid was dried under vacuum. The fruit extract and dried powder were analyzed by Fourier transform infra-red spectroscopy (IR-Prestige 22, Shimadzu) in order to identify the biomolecules responsible for reduction and stabilization.

### 2.2.3. Study of antimicrobial activity of Ag-nanoparticles

The antimicrobial activity of the Ag nanoparticles was studied against three common bacteria and two fungi using conventional disc diffusion method. Bacteria cultures were maintained on nutrient agar media whereas fungal cultures were maintained on potato dextrose agar. Pure apple fruit extract was used as a control for comparison of results. The fruit extract and suspension of Ag-nanoparticles were added separately into two different cups made on each plate seeded with organism. Then the organisms were allowed to grow inside an incubator at proper temperature under dark condition for a certain period. The antimicrobial activity was evaluated by observing and measuring the zone of inhibition around the cups.

## 3. Results and Discussion

### 3.1 UV-Vis Spectrophotometry

The fruit extract appears to be a potential source of water soluble hydrocarbons, proteins those are found to be efficient reducer and stabilizer for nanoparticles. UV-Vis spectrophotometer

was used to examine the formation and stability of the Ag nanoparticles in the aqueous colloidal solution. After 3 hours of adding the extract to the silver nitrate solution at room temperature, color of the solution started to change from light yellow to brown indicating the formation of Ag nanoparticles (31). The color of the solution became darker with time and turned into dark brown after 24 hours as shown in Figure 2. It was emphasized from previous studies that the color of nanoparticles originates from excitation of the surface plasmon resonance that generally depends on the size, shape of the nanoparticles, chemical surrounding adsorbed species, dielectric constant etc (32-35). Absorption spectra of the Ag nanoparticles, recorded at different time interval (3, 6, 12, 18, 24 and 28 hours), are presented in Figure 3a. It is clear from figure that each absorption spectrum consists of a peak that corresponds to characteristic surface plasmon peak of Ag nanoparticles. Careful analysis shows that the absorption peak corresponding to Ag nanoparticle, prepared during 6, 9 and 12 hours are measured at 441 nm whereas this is noticed at 447 and 450 nm for nanoparticles prepared at 18 and 24 hours of reaction time. Such red shift in the absorption peak might be due to increase in the particle size (36, 37). A tail in the longer wavelength region of the absorption spectra corresponds to the size and shape distribution of the synthesized Ag nanoparticles (38). The appearance of the second peak at 380 nm that steadily builds up with reaction time may also assigned to another surface plasmon resonance peak of Ag nanoparticles (39-41). 3a (inset) figure depicts the variation of absorption maxima with reaction time. It may be concluded from figure that the absorption of Ag nanoparticles increases linearly with time upto 18 hours of reaction time then it saturates. The increase of the absorption may be due to either increase of the number of particles or due to increasing volume of the nanoparticles. Since the position of absorption maxima does not change significantly between 6 and 18 hours, so we may conclude that the enhancement of the absorption maxima originates from increasing number of nanoparticles. Beyond 18 hours of reaction time, increase in the absorption maxima is associated with the red shift of the plasmon frequency. So the enhancement of the absorption maxima may be assigned with increasing size of the Ag nanoparticles. The absorption maxima of the sample did not change beyond 24 hours of reaction time. Thus completion of the reaction can be concluded from such behavior of the absorbance maximum during this time interval (31).

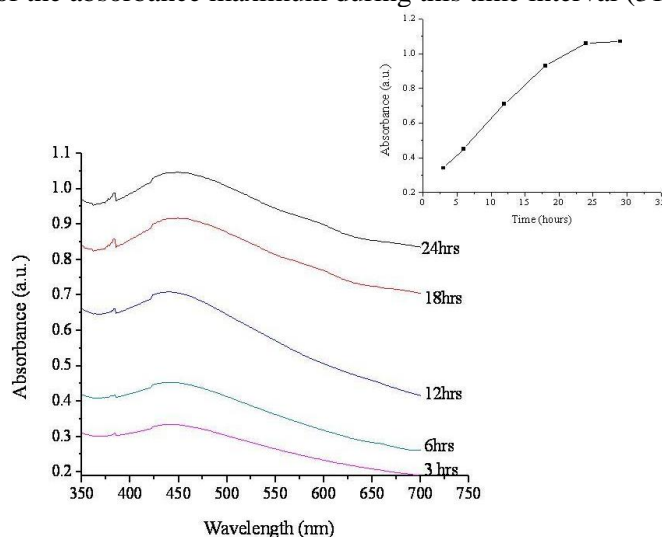


Fig. 3(a). UV-Vis absorption spectra of the mixture at different time interval (for a specific concentration 10 mM). Inset figure shows variation of absorbance of mixture with time

In order to gain more insight about the dependence of the reaction rate upon concentration of  $\text{AgNO}_3$  solution, we have also taken the absorption spectra of aqueous solution containing different amount of  $\text{AgNO}_3$  maintaining fixed time of reaction. In Figure 3b, we have plotted UV-Vis spectra of the aqueous solution containing different concentration of  $\text{AgNO}_3$  (3, 5, 10, 15 mM). Peak position does not change with increasing  $\text{AgNO}_3$  concentration, thus it may be concluded that the particle size does vary significantly with concentration during this time interval. 3b (inset) figure shows the variation of maximum absorbance with  $\text{AgNO}_3$  concentration. It is

clear that the absorbance maxima increases almost linearly with  $\text{AgNO}_3$  concentration i.e. formation of Ag nanoparticles increases linearly with  $\text{AgNO}_3$  concentration.

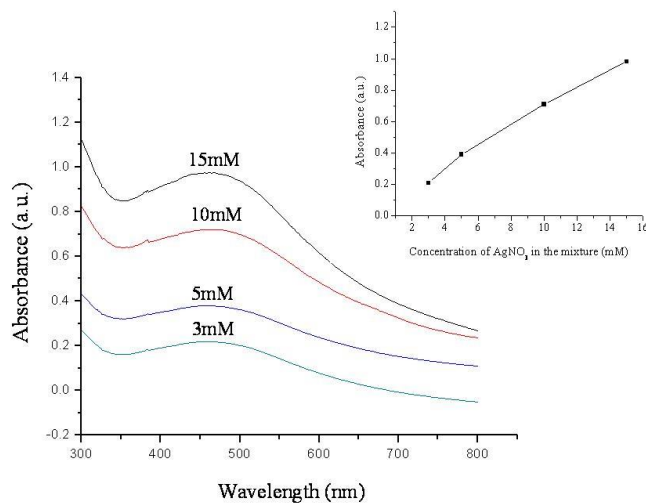


Fig. 3(b). UV-Vis absorption spectra of the mixture with different  $\text{AgNO}_3$  concentration (measured after 12 hours of mixing). Inset figure shows variation of absorbance maxima with  $\text{AgNO}_3$  concentration

### 3.2 X-ray Diffraction

One typical x-ray diffraction pattern of the as-prepared precipitate, collected after 6 hours of reaction time, consists of six diffraction peaks centered at  $2\theta = 32.04^\circ$ ,  $38.02^\circ$ ,  $43.96^\circ$ ,  $46.1^\circ$ ,  $64.14^\circ$  and  $77.64^\circ$  and can readily be indexed as (122), (111), (200), (231), (220) and (311) planes for face centered cubic structures of silver (Figure 4; JCPDS: File No. 4-783). It is interesting to note that all these diffraction peaks match very well not only with their respective peak positions but also with their relative peak intensities. It can be concluded that the presence of no peak other than the characteristic peaks in the diffraction pattern confirms the purity and crystallinity of the as-prepared Ag nanoparticles.

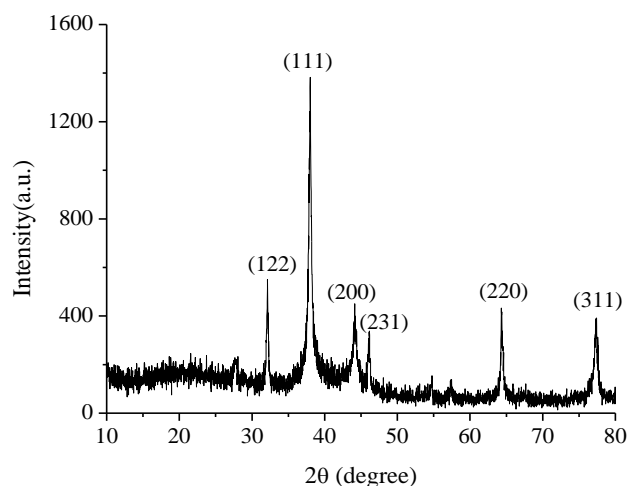


Fig. 4. X-ray diffraction pattern of the biosynthesized Ag nanoparticles

### 3.3 Transmission Electron Microscopy

The microstructure and crystallinity of the as-prepared Ag nanoparticles was also examined by high-resolution transmission electron microscope (HRTEM). Figure 5 (a – c) show

typical TEM image of Ag nanoparticles prepared using fruit extract of apple. It is clear from TEM images that the as-prepared Ag nanoparticles possess spherical shape with diameter of 20 nm. The lattice fringes (Figure 5d) depict that the internal structure of the particles is highly crystallized. The interplanar spacing is calculated to be 0.235 nm that corresponds to the (111) planes of face centered cubic phase of Ag nanoparticles.

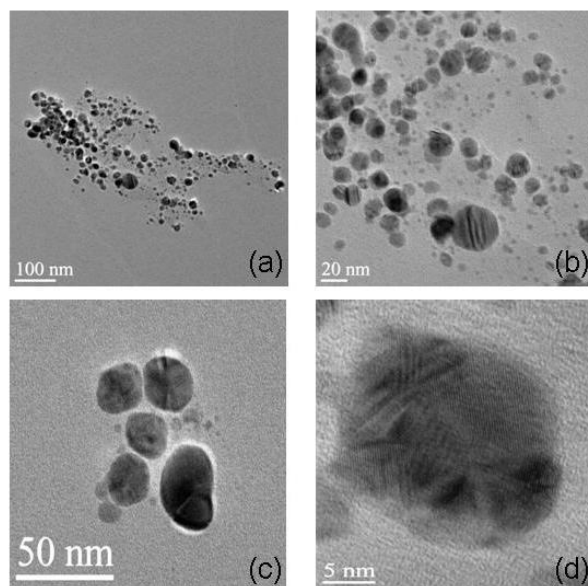


Fig. 5. TEM images of Ag nanoparticles synthesized by using apple extract

### 3.4 FTIR Spectroscopy

Fourier transform infrared (FTIR) spectroscopy was employed to detect the biomolecules responsible for reduction and stabilization of silver ions. The FTIR spectra of apple extract and biosynthesized Ag nanoparticles, measured in absorption mode, are shown in Figure 6. The spectrum of apple extract consists of several bands at 542, 687, 785, 835, 1167, 1266, 1479, 1672, 2144, 2778, 3588  $\text{cm}^{-1}$ . Bands 542 and 1672  $\text{cm}^{-1}$  correspond to amide-I (42, 43) whereas band at 1479  $\text{cm}^{-1}$  originates from amide linkage (44). Specifically the band appearing at 1672  $\text{cm}^{-1}$  corresponds to the  $-\text{C}=\text{O}-$  stretching vibration modes of tertiary amides coupled with C-N stretch, C-N deformation and in-plane N-H bending (45, 46). Band at 1167 and 1266  $\text{cm}^{-1}$  denote phenolic group of aromatic compounds (47) and C-O stretching mode vibration (48) respectively. Bands near 2144 and 3588  $\text{cm}^{-1}$  can be assigned to C=C stretching vibration (45) and intermolecular hydrogen bonded network of  $-\text{OH}$  or  $-\text{NH}$  group (49) respectively. The broad band at 2778  $\text{cm}^{-1}$  originates from C-H vibration (50). In the low energy region, two bands at 687 and 785  $\text{cm}^{-1}$  indicates the presence of hydrocarbons (51, 52) and aromatic rings (53) respectively. Since, previous studies revealed that the presence of high percentage of ascorbic acid within apple extract (54, 55), we may conclude that the FTIR spectrum of  $-\text{C}-\text{O}-$ ,  $-\text{C}=\text{O}-$  may have contribution from ascorbic acid as well. So from above analysis, we may conclude that protein and ascorbic acid present in apple extract plays a major role to reduce  $\text{Ag}^+$  ion into metallic Ag nanoparticles.

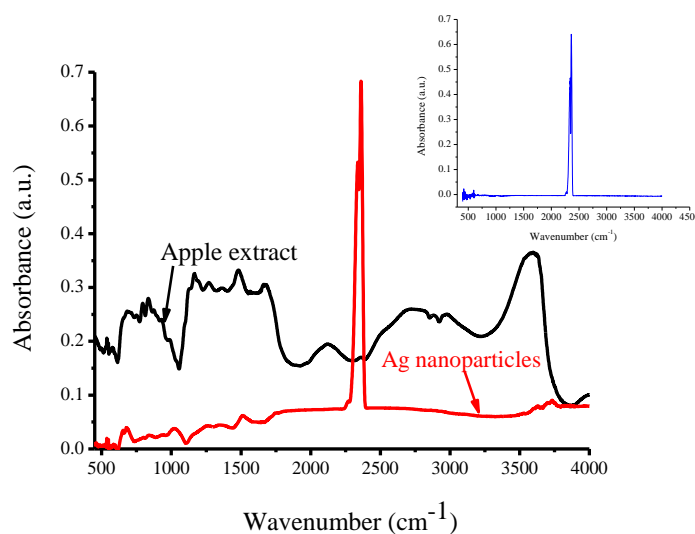


Fig. 6. FTIR spectra of apple fruit extract and biosynthesized silver nanoparticles  
Inset curve shows the spectrum for bare substrate

The biosynthesized silver nanoparticles show high level of purity as the FTIR spectrum of the Ag-nanoparticles didn't show any distinct bands throughout the entire range of IR-spectrum. However, high resolution spectrum shows that there are few bands at 531, 669, 1018, 1516, 2360, 3735  $\text{cm}^{-1}$  (Figure. 6). The first band originates from Ag nanoparticle - ligand stretching vibration that appears due to interaction of biomolecules with nanoparticles (56). The bands at 669 and 1516  $\text{cm}^{-1}$  may be ascribed to vibrational energy of aromatic hydrocarbons and amide linkage those have possessed their energy changed due to interaction with nanoparticles. The bands at 1018 and 3735  $\text{cm}^{-1}$  originate from anti-symmetric  $\text{-C-O-}$  vibration (57) and  $\text{-OH}$  stretching of protein molecules (56) respectively. A sharp peak at 2360  $\text{cm}^{-1}$  generates from the instrumental error and hence it may be ignored (shown in the inset of Figure 6). Thus from analysis of the FTIR spectrum of Ag nanoparticle, we may conclude that the amide and hydrocarbon present in apple extract stabilize the Ag nanoparticles.

### 3.5 Analysis of antibacterial and antifungal activity

In vitro antibacterial activity of Ag nanoparticles was agar disc diffusion assay method. Here, antibacterial activity of the synthesized Ag nanoparticles was studied against three bacteria: one gram positive bacterium - *Staphylococcus aureus* that causes variety of infections in human bodies like skin lesions, mastitis, phlebitis etc. (58) and two gram negative bacteria - *Klebsiella pneumoniae* and *Escherichia coli*. *Klebsiella pneumoniae* is responsible urinary tract infection, septicemia, pyogenic infections etc., on the other hand *Escherichia coli* causes infections like neonatal meningitis, gastroenteritis etc. in human system (58). After incubation of these bacterial strains for 24 hours in dark at 37°C, distinct zones of inhibition were observed around the cups, impregnated with Ag nanoparticles (shown in Figure 7). This observation suggests strong antibacterial activity of our synthesized Ag nanoparticles (59). No zone of inhibition was noticed when only fruit extract of apple was added, which suggests that the apple fruit extract doesn't possess antibacterial property against these three bacteria. Figure 7 shows the prevented growth of all the three bacteria to different levels in the presence of silver nanoparticles. Highest activity has been noticed against *Escherichia coli* having zone of inhibition 13.10 mm whereas zone of inhibition against two other bacteria - *Klebsiella pneumoniae* and *Staphylococcus aureus* are found to be 12.92 and 12.75 mm respectively. Our observed zone of inhibition against *Staphylococcus aureus* is found to be greater than that of plant mediated Ag-nanoparticle examined by M.S. Abdel-Aziz et al (zone of inhibition ~ 12.63 mm, 26). Very recently, M. Ghaffari-Moghaddam *et al.* reported the zone of inhibition 9 mm and 13 mm of *Crataegus douglasii* fruit extract mediated Ag-nanoparticles against *Escherichia coli* and *Staphylococcus aureus* respectively (37). It may be

emphasized from the previous studies that the zone of inhibition of gram negative bacteria possesses higher value than that of gram positive bacteria due to differences in their membrane structure (31, 50). It is believed from past studies that the high bactericidal activity of Ag nanoparticles originates from released Ag cations from Ag nanoparticles (60). These Ag cations are attracted towards bacteria cell due to negative charge on their surfaces and are attached on cell. Then they cause a change in the membrane permeability of the bacteria cell that leads to cell death (61-64).

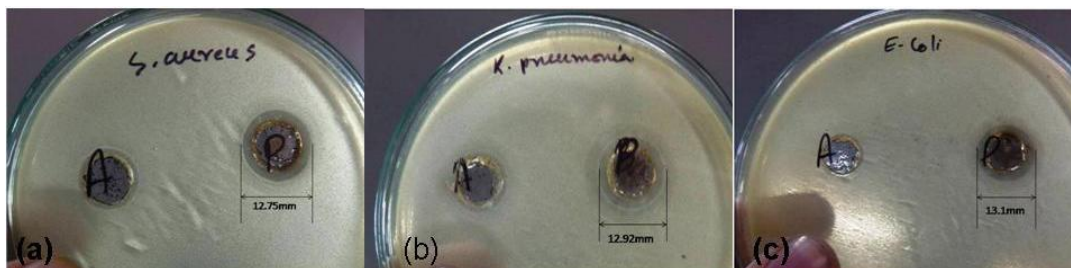


Fig. 7 Zone of inhibition observed against (a)*S. aureus*, (b)*K. pneumoniae* and (c)*E. coli*

Similar to antibacterial activity, we have also tested antifungal activity of our biosynthesized silver nanoparticles against two fungi namely *Aspergillus niger* and *Aspergillus wentii*. After pouring the suspensions into the cups, the strains were incubated at 30°C in dark. After 48 hours of incubation, we observed zone of inhibition around the cups where suspension of Ag nanoparticle was added. Here also, the pure fruit extract was found to be unable to prevent the growth of fungi. We measured zone of inhibition 11.50 and 11.83 mm for *Aspergillus niger* and *Aspergillus wentii* respectively (not shown here). The zone of inhibition against different bacteria and fungi are summarized in Figure 8.

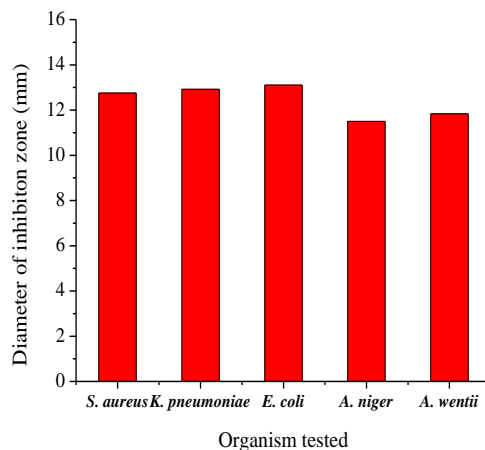


Fig. 8. Graph shows the activity of Ag-nanoparticles against three bacteria and two fungi (diameters were taken as mean of triplicates)

#### 4. Conclusion

Our objective was to synthesize metallic nanoparticles by a simple and eco-friendly procedure unlike chemical methods. We screened and tested a lot of fruits whose extract might act as a reducing agent to synthesize Ag nanoparticles from aqueous solution of silver nitrate. Among all these fruits, apple was found to be a good choice due to its high content of organic reducing agents. The fruit extract of apple reduced the silver ions and produced metallic silver nanoparticles with well-defined stability. These nanoparticles were closely spherical in shape and the average particle size was found to be 20 nm. The antimicrobial study revealed that these biosynthesized silver nanoparticles have inhibitory effect on bacteria and fungi as well. This simple and 'green'



procedure may be scaled up for large scale production of metal nanoparticles due to its economical viability.

### Acknowledgement

One of the authors (K. Roy) thanks the Council of Scientific and Industrial Research for providing financial assistance (Senior Research Fellowship).

### References

- [1] R. Das, S.S. Nath, D. Chakdar, G. Gope, R. Bhattacharjee, *J. Exp. Nanosci.* **5**(4), 357 (2010)
- [2] M. Bhaumik, H.J. Choi, R.I. McCrindle and A. Maity, *J. of Colloid Interf. Sci.* **425**, 75 (2014)
- [3] D. Chen, X. Qiao, X. Qiu and J. Chen, *J. Mater. Sci.* **44**(4), 1076 (2009)
- [4] M. Rai, A. Yadav and A. Gade, *Biotechnol. Adv.* **27**(1), 76 (2009)
- [5] B.D. Gusseme, L. Sintubin, L. Baert, E. Thibo, T. Hennebel, G. Vermeulen, M. Uyttendaele, W. Verstraete and N. Boon, *Appl Environ Microbiol.*, 76(4), 1082 (2010)
- [6] M.V. Cañamares, J.V. Garcia-Ramos, S. Sanchez-Cortes, M. Castillejo, M. Oujja, *J. Colloid Interf. Sci.* **326**, 103 (2008)
- [7] M.V. Roldán, N. Pellegrini, O. de Sanctis, *J. Nanoparticles*, Article ID 524150, 7 pages (2013)
- [8] J.C. Scaiano, P. Billone, C.M. Gonzalez, L. Maretti, M.L. Marin, K.L. McGilvray, N. Yuan, *Pure Appl. Chem.*, **81**(4), 635 (2009)
- [9] R.K. Swarnkar, S.C. Singh and R. Gopal, *Bull. Mater. Sci.*, **34**(7), 1363 (2011)
- [10] B. Wang, X. Zhuang, W. Deng and B. Cheng, *Sci. Res. Eng.*, **2**(5), 387 (2010)
- [11] J.T. Huang, X.X. Yang, Q.L. Zenga and J. Wang, *Analyst*, **138**, 5296 (2013)
- [12] S.P. Chandran, M. Chaudhary, R. Pasricha, A. Ahmad and M. Sastry, *Biotechnol Prog.* **22**(2), 577 (2006)
- [13] S.S. Shankar, A. Rai, A. Ahmad and M. Sastry, *J. Colloid Interf. Sci.* **275**, 496 (2004)
- [14] S.S. Sudha, K. Rajamanickam and J. Rengaramanujam, *Indian J. Exp. Biol.*, **52**, 393 (2013)
- [15] M. Gajbhiye, J. Kesharwani, A. Ingle, A. Gade and M. Rai, *Nanomed-Nanotechnol.*, **5**(4), 382 (2009)
- [16] A. Syed, S. Saraswati, G.C. Kundu, A. Ahmad, *Spectrochim. Acta A*, **114**, 144 (2013)
- [17] K. Vahabi, G.A. Mansoori and S. Karim, *Insciencas J.*, **1**(1), 65 (2011)
- [18] C. Malarkodi, S. Rajeshkumar, K. Paulkumar, G. Gnanajobitha, M. Vanaja and G. Annadurai, *Nanosci. Nanotech.*, **3**(2), 26 (2013)
- [19] A. Prakash, S. Sharma, N. Ahmad, A. Ghosh & P. Sinha, *J. Biomater. Nanobiotech.*, **2**, 156 (2011)
- [20] S. Seshadri, A. Prakash and M. Kowshik, *Bull. Mater. Sci.*, **35**(7), 1201 (2012)
- [21] S. Yasin, L. Liu and J. Yao, *J. Fiber Bioeng. Inform.*, **6**(1), 77 (2013)
- [22] J.Y. Song and B.S. Kim, *Bioprocess Biosyst Eng.*, **32**, 79 (2009)
- [23] A.I. Lukman, B. Gong, C. Marjo, U. Roessner & A.T. Harris, *J. Colloid Interf. Sci.* **353**, 433 (2011)
- [24] V.R. Pasupuleti, T.N.V.K.V. Prasad, R.A. Shiekh, S.K. Balam, G. Narasimhulu, C.S. Reddy, I.A. Rahman and S.H. Gan, *Int. J. Nanomed.*, **8**, 3355 (2013)
- [25] H. Lee, J.Y. Song and B.S. Kim, *J. Chem. Tech. Biot. B.* **88**(11), 1971 (2013)
- [26] M.S. Abdel-Aziz et al., *J. Saudi Chem. Soc.*, <http://dx.doi.org/10.1016/j.jscs.2013.09.011> (2013)
- [27] T. Elavazhagan and K.D. Arunachalam, *Int. J. Nanomed.*, **6**, 1265 (2011)
- [28] K. Roy, S. Biswas and P.C. Banerjee, *Res. J. Pharm. Biol. Chem. Sci.*, **4**(1), 1271 (2013)
- [29] D. Jain, H.K. Daima, S. Kachhwaha and S.L. Kothari, *Dig. J. Nanomater. Bios.*, **4**(4), 723 (2009)
- [30] R.S. Rimal Isaac, G. Sakthivel, and Ch. Murthy, *J. Nanotech.*, Article ID 906592, 6 pages (2013)

- [31] P. Prakasha, P. Gnanaprakasama, R. Emmanuela, S. Arokiyarajb, M. Saravanan, *Colloid. Surf. B*, **108**, 255 (2013)
- [32] P. Mulvaney, *Langmuir*, **12**, 788 (1996)
- [33] T.C.R. Rocha, H. Winischhofer, E. Westphal and D. Zanchet, *J. Phys. Chem, C*- **111**, 2885 (2007)
- [34] Y. Xiong, I. Washio, J. Chen, H. Cai, Z.Y. Li and Y. Xia, *Langmuir*, **22**, 8563 (2006)
- [35] J. Chen, B.J. Wiley and Y. Xia, *Langmuir* **23**, 4120 (2007)
- [36] J. J. Mock, M. Barbic, D.R. Smith, D.A. Schultz & S. Schultz, *J. Chem. Phys*, **116**(15), 6755 (2002)
- [37] M. Ghaffari-Moghaddam and R. Hadi-Dabanlou, *J. Indus. Eng. Chem.*, **20**, 739 (2014)
- [38] N. Vigneshwaran, A.K. Kathe, P.V. Varadarajan, R.R. Nachane, R.H. Balasubramanya, *Colloid. Surf. B*, **53**, 55 (2006)
- [39] R. He, X. Chian, J. Yin and Z. Zhu, *J. Mater. Chem.*, **12**, 3783 (2002)
- [40] N.A. Begum, S. Mondal, S. Basu, R.A. Laskar, D. Mondal, *Colloid. Surf. B*, **71**, 113 (2009)
- [41] J. Xie, J.Y. Lee, D.I.C. Wang and Y.P. Ting, *ACS Nano*, **1**, 429 (2007)
- [42] L.R. Jaidev and G. Narasimha, *Colloid. Surf. B*, **81**(2), 430 (2010)
- [43] G. Chen, B. Ying, G. Zeng, Q. Niu, M. Yan, A. Chen, J. Du, J. Huang and Q. Zhang, *Colloid. Surf. B*, **117**, 199 (2014)
- [44] K. Kalishwaralal, V. Deepak, S. R. K. Pandian, M. Kottaisamy, S. B. M. Kanth, B. Karthikeyan and S. Gurunathan, *Colloid. Surf. B*, **77**, 257 (2010)
- [45] R. Sathyavathi, M. Balamurali Krishna, S. Venugopal Rao, R. Saritha, D. Narayana Rao, *Adv. Sci. Lett.*, **3**,1 (2010)
- [46] O.S. Oluwafemi, Y. Lucwaba, A. Gura, M. Masabeya, V. Ncapayi, O.O. Olujimi, S.P. Songcab, *Colloid. Surf. B*, **102**, 718 (2013)
- [47] A. M. Fayaz, M. Girilal, R. Venkatesan and P.T. Kalaichelvan, *Colloid. Surf. B*, **88**, 287 (2011)
- [48] C.H. Ramamurthy, M. Padma, I.D. Mariya Samadanam, R. Mareeswaran, A. Suyamvaram, M.S. Kumar, K. Premkumar and C. Thirunavukkarasu, *Colloid. Surf. B*, **102**, 808 (2013)
- [49] M. Annadhasan, V.R.S. Babu, R. Naresh, K.U. Maheswari and N. Rajendran, *Colloid. Surf. B*, **96**, 14 (2012)
- [50] V. Gopinath, M. Ali, S. Priyadarshini, N. M. Priyadarshini, N. Thajuddin and P. Velusamy, *Colloid. Surf. B*, **96**, 69 (2012)
- [51] P. Kumar, M. Govindaraju, S. Senthamilselvi and K. Premkumar, *Colloid. Surf. B*, **103**, 658 (2013)
- [52] K.L. Niraimathi, V. Sudha, R. Lavanya and P. Brindha, *Colloid. Surf. B*, **102**, 288 (2013)
- [53] A. Mishra, N.K. Kaushik, M. Sardar and D. Sahal, *Colloid. Surf. B*, **111**, 713 (2013)
- [54] J. Wawrzyniak, A. Ryniecki and W. Zembrzuski, *Acta Sci. Pol.-Technol.*, **42**(2), 5 (2005)
- [55] A.M. Pisoschi, A.F. Danet and S. Kalinowski, *J. Autom. Method. Manag.*, Article ID 937651, 8 pages, <http://dx.doi.org/10.1155/2008/937651> (2008)
- [56] T. Ahmad, Y.A. Wani, N. Manzoor, J. Ahmed and A.M. Asiri, *Colloid. Surf. B*, **107**, 227 (2013)
- [57] A. Annamalai, V.L.P. Christina, D. Sudha, M. Kalpana and P.T.V. Lakshmi, *Colloid. Surf. B*, **108**, 60 (2013)
- [58] T.V. Mathew and S. Kuriakose, *Colloid. Surf. B*, **101**, 14 (2013)
- [59] A. Panáček, L. Kvítek, R. Prucek, M. Kolář, R. Večeřová, N. Pizúrová, V.K. Sharma, T. Nevěčná and Radek Zbořil, *J. Phys. Chem. B*, **110**(33), 16248 (2006)
- [60] S. Priyadarshini, V. Gopinath, N.M. Priyadarshini, D.M. Ali and P. Velusamy, *Colloid. Surf. B*, **102**, 232 (2013)
- [61] P. Dibrov, J. Dzioba, K.K. Gosink and C.C. Hase, *Antimicrob. Agents Chemother.*, **46**, 2668 (2002)
- [62] I. Sondi and B. Salopek-Sondi, *J. Colloid. Interf. Sci.*, **275**, 177 (2004)
- [63] Lin Y.E., Vidic R.D., Stout J.E., McCartney C.A. and Yu V.L. *Water Research*, **32**(7), 1997 (1998)
- [64] P.K. Stoimenov, R.L. Klinger, G.L. Marchin and K.J. Klabunde, *Langmuir*, **18**(17), 6679 (2002)